

Oblate collectivity in ^{197}Pb

A. Kuhnert, M. A. Stoyer, J. A. Becker, E. A. Henry, M. J. Brinkman, S. W. Yates,* and T. F. Wang
Lawrence Livermore National Laboratory, Livermore, California 94550

J. A. Cizewski
Rutgers University, New Brunswick, New Jersey 08903

F. S. Stephens, M. A. Deleplanque, R. M. Diamond, A. O. Macchiavelli,† J. E. Draper,‡ F. Azaiez,§
W. H. Kelly,** and W. Korten††
Lawrence Berkeley Laboratory, Berkeley, California 94720

(Received 7 February 1992)

Evidence for collective behavior in the high-spin region of lead nuclei is provided by the observation of two collective structures in ^{197}Pb . One of these bands is interpreted as an oblate collective structure built on oblate proton and possibly neutron states. A second more irregular band is suggested to be most likely a triaxial rotational band. Neutron and proton configurations for these bands are suggested from the results of quasiparticle Routhians and total Routhians surface calculations. A partial level scheme up to $I \approx \frac{69}{2}$ and $E_x \approx 8$ MeV is presented.

PACS number(s): 21.10.Re, 21.60.Ev, 27.80.+w

I. INTRODUCTION

The discovery of the superdeformed (SD) bands in nuclei near $A = 192$ [1–4], and the continuing search for additional SD bands has resulted in extensive gamma-gamma coincidence data for several nuclei in this region. These coincidence data were analyzed in order to extend the yrast line of the first-well states, and to look for predicted collective behavior in these nuclei. We report here the observation of at least two new bands in ^{197}Pb [5]. One of the bands is an irregularly spaced structure of 20 intense dipole transitions ($\Delta I = 1$) with transition energies between 126 and 432 keV and seven weak $\Delta I = 2$ crossover transitions. A second band is more regular, and consists of eight intense dipole transitions with two $\Delta I = 2$ crossover transitions.

The yrast states with spin $I \leq 12\hbar$ in the known light lead isotopes ($A \approx 196$) are of two-quasineutron character. States of higher I are built on four and more quasiparticles [6]. However, there is also evidence for collective behavior. Low-lying 0^+ states have been found in the neutron-deficient, even-mass lead isotopes [7] and $8^+, 11^-$ isomeric states are seen in $^{194,196}\text{Pb}$ [8–10]. In

^{196}Pb a collective band built on the low-lying 0^+ state has been observed [9]; however, the structure is disturbed by an 8^+ isomer. These low-lying isomeric $0^+, 8^+$, and 11^- states are explained as oblate, proton states having the two-particle-two-hole (2p-2h) configurations $\pi(+\frac{1}{2}[400]^{-2}; \frac{9}{2}^{-}[505]^2)_{0^+,8^+}$ and $\pi(\frac{1}{2}^+[400]^{-2}; \frac{9}{2}^{-}[505]; \frac{13}{2}^+[606])_{11^-}$, respectively [11], rather than two-quasineutron configurations.¹ Indeed, oblate minima have been predicted [7,12,13] for the light lead isotopes at $\gamma \approx -60^\circ$ and $\beta_2 \approx 0.17$. The observed bands in ^{197}Pb , similar to the irregular band in ^{194}Pb [10], to the recently published regular bands in ^{198}Pb [14,15], $^{199,200}\text{Pb}$ [16], and to the collectively rotating oblate bands in the $A = 130$ region [17], are thus candidates as rotational bands built on oblate proton states. In Sec. II we give a short summary of the experiments used to obtain the data, in Sec. III we shall discuss the results of the data analysis, and in Sec. IV we compare the experimental results with the theoretical calculations. A summary is given in Sec. V.

II. EXPERIMENT

The experiments have been done at the Lawrence Berkeley Laboratory 88-Inch Cyclotron using the high-energy-resolution array (HERA), which consists of 20 Compton-suppressed Ge detectors and a 4π inner ball of 40 BGO detectors. The data presented here have been obtained using the two fusion evaporation reactions,

*Permanent address: University of Kentucky, Lexington, KY 40506.

†Permanent address: Comision Nacional de Energia Atomica, Buenos Aires, Argentina.

‡Permanent address: University of California, Davis, CA 95616.

§Permanent address: IPN-Orsay, F-91406, Orsay, France.

**Permanent address: Iowa State University, Ames IA 50011.

††Present address: Niels Bohr Institute, Copenhagen, Denmark.

¹The oblate-driving proton orbitals are the same as those mentioned in Refs. [7–10]. They are labeled correctly here but mislabeled in these references. Apparently a misprint in an earlier reference was propagated throughout Refs. [7–10].

$^{176}\text{Yb}(^{26}\text{Mg}, 5n)^{197}\text{Pb}$ at $E(^{26}\text{Mg})=135$ MeV and $^{154}\text{Sm}(^{48}\text{Ca}, 5n)^{197}\text{Pb}$ at $E(^{48}\text{Ca})=210$ MeV. The targets consisted of three and two stacked foils, respectively, each foil ≈ 500 $\mu\text{g}/\text{cm}^2$ thick. All threefold and higher-fold coincidences were recorded together with the sum-energy (H) and multiplicity (K) information from the inner BGO ball. Twofold events have been recorded only when at least four inner ball detectors were in prompt coincidence with the two Ge detectors. Approximately 4.5×10^8 double coincidences (including resolved higher-fold events) were collected in the ^{26}Mg beam bombardment and about 2.2×10^8 coincidences in the ^{48}Ca bombardment.

III. RESULTS

The analysis of the twofold coincidence data resulting from the ^{48}Ca bombardment yielded one irregular and six regular bands. The irregular band and five of the six regular bands were also found in the ^{26}Mg data. The remaining regular band is already assigned to ^{198}Pb and will be discussed in detail elsewhere [15]. The irregular and two of the regular bands could be assigned unambiguously to ^{197}Pb due to the fact that they are in coincidence with the known low-lying transitions in ^{197}Pb . An unambiguous isotopic assignment for the other three bands is not yet possible, although one of the bands shows weak coincidences with known transitions in ^{196}Pb . In this paper we shall only discuss the properties of the two strongest bands in ^{197}Pb (one of the regular bands and the irregular band).

Figure 1 shows the evidence for the regular band to-

gether with the low-lying coincident ^{197}Pb yrast transitions. The band members are eight strong, nearly evenly spaced, transitions in the energy range between 100 and 500 keV. Known transitions in ^{197}Pb are marked with arrows. Figure 2 illustrates a partial level scheme of ^{197}Pb with the transition intensities (indicated values include the calculated internal electron conversion contributions) determined from a spectrum coincident with the 200.5-keV transition. The intensity for the 200.5-keV transition has been determined in a spectrum coincident with the 150.8-keV transition normalized to the intensity of the 266.2-keV transition. The left-hand side in Fig. 2 includes the known isomeric levels in ^{197}Pb [6] and levels populated only in the decay of these isomers. Since γ -ray coincidence detection across these isomers is strongly suppressed in our experimental arrangement, the transitions below these isomers were not observed. The excitation energy of the regular band has not been determined thus far because candidates for linking transitions to the low-lying levels in the energy range of 300–500 keV have not been placed unambiguously. However, based on the intensities of the low-lying transitions measured in coincidence with the 200.5-keV transition, the most likely depopulation pattern for the band is indicated by dashed arrows in Fig. 2. The 112-keV transition is in coincidence with all of the transitions in the regular band, but it carries only 35(4)% of the band intensity (Fig. 2). This is, within the uncertainties, a value consistent with the observed intensities of the low-lying transitions in coincidence with the band (see Fig. 1). Therefore, the level from which the 112.3-keV transition originates is either isomeric (i.e., coincidence detection is suppressed) or

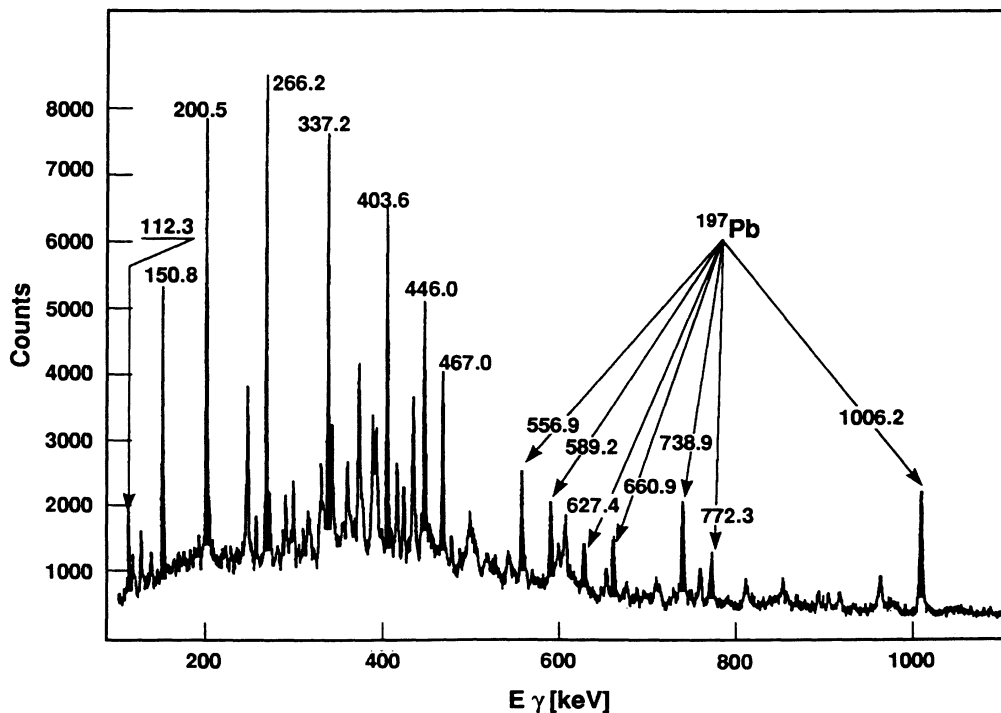


FIG. 1. Sum of gamma-coincidence spectra (energy gates on all eight transitions in the regular band in ^{197}Pb). The arrows mark the known low-lying transitions in ^{197}Pb .

$\approx 65\%$ of the band intensity decays out of this level, perhaps, e.g., into the $\frac{33}{2}$ isomer. However, the DCO ratio (directional correlation of γ transitions from oriented nuclei) and the γ -ray intensity yield ratio R (see text below) do not seem to be consistent with an isomeric bandhead.

The spectrum of the irregular band is shown in Fig. 3, together with a coincident known transition (557 keV) in ^{197}Pb . The irregular pattern of transition energies and in-

tensities for the marked band members is immediately apparent. A partial level scheme for this band, based on our present analysis, is shown in Fig. 4. The transition intensities indicated in Fig. 4 (corrected for calculated internal conversion) are taken from a spectrum coincident with the 432.7-keV transition. The intensity of the 432.7-keV transition was determined from a spectrum coincident with the 152.4-keV transition, normalized to the 270.4-keV transition intensity. Again, linking transi-

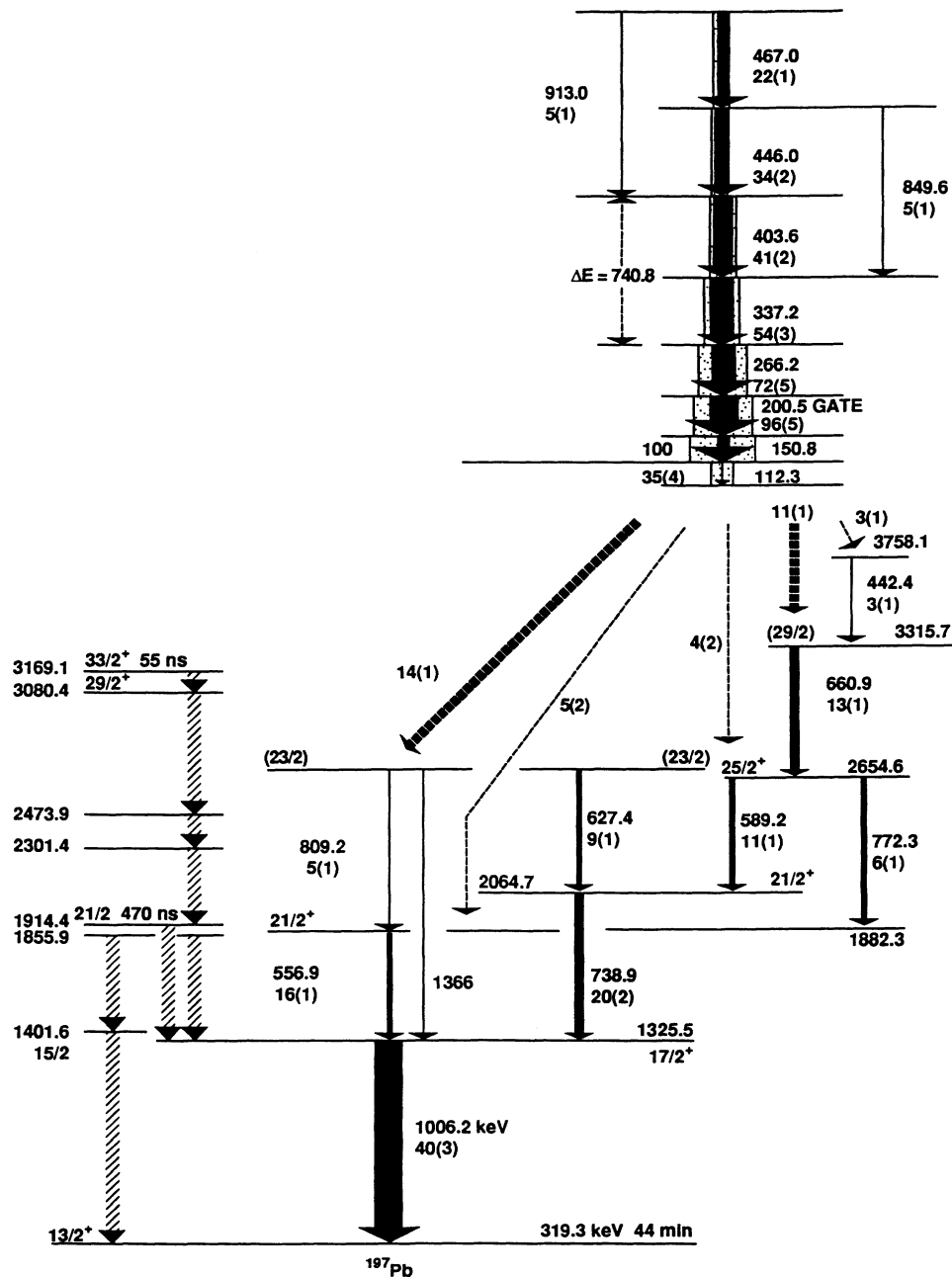


FIG. 2. Partial level scheme for ^{197}Pb showing the most likely population of the low-lying levels by the regular band. The energies are in keV with uncertainties of 0.1 keV for the strong transitions and up to 0.4 keV for the weakest ones. Full arrows are proportional to γ -transition intensity, and the dotted backgrounds are proportional to transition strength including the calculated internal electron conversion contributions. The intensities are taken from a coincidence spectra gated on the 200.5-keV transition.

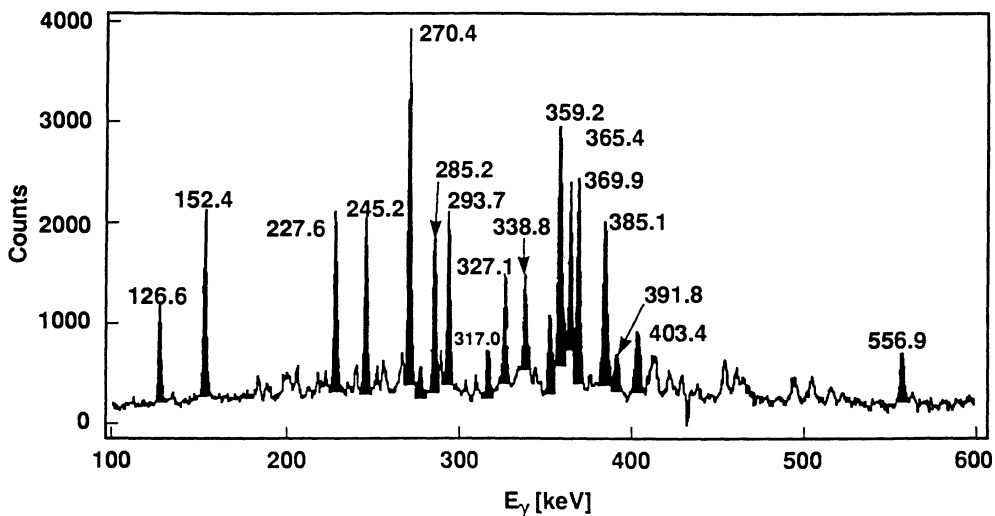


FIG. 3. Gamma-coincidence spectrum with an energy gate on the 432-keV member of the irregular band. The 556.9-keV transition is a known low-lying transition in ^{197}Pb .

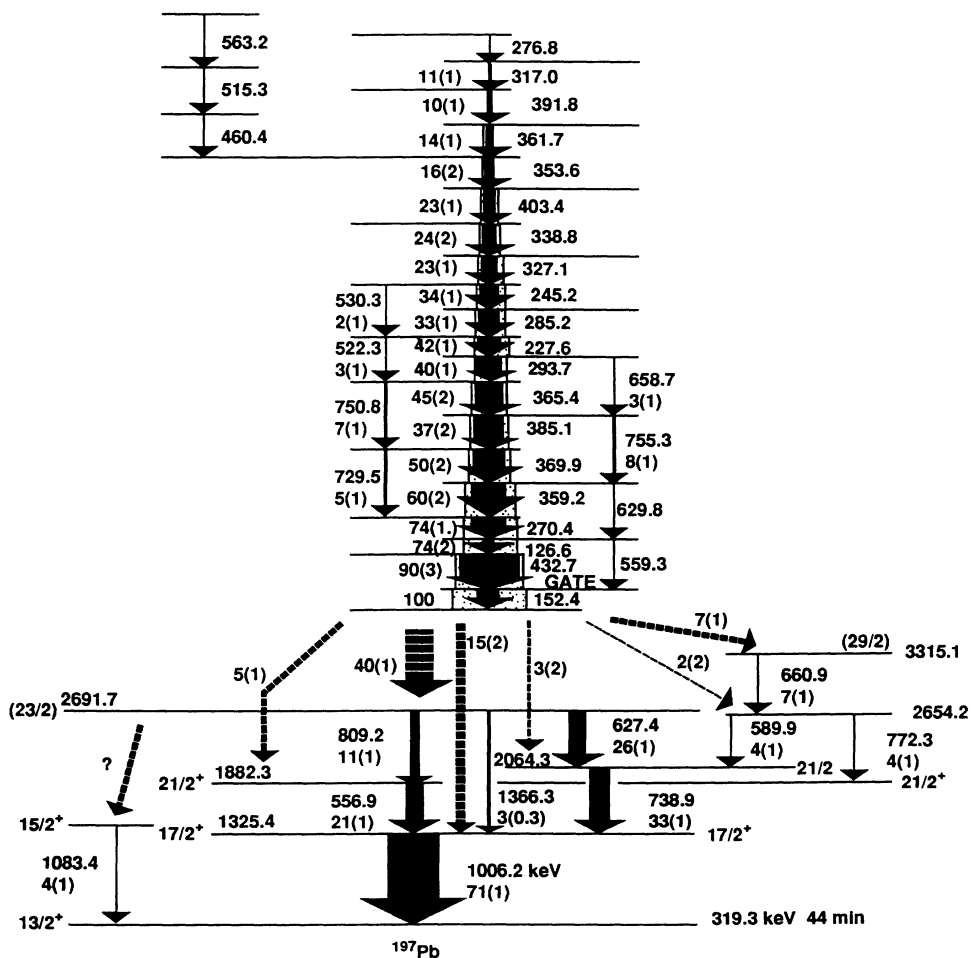


FIG. 4. Same as Fig. 2 but for the irregular band in ^{197}Pb . Intensities from a coincidence spectrum are gated on the 432.7-keV transition.

tions to the low-lying states have not been found, and the dashed arrows in Fig. 4 show the most likely depopulation pattern for this irregular band. About 75(1.5)% of the band intensity is observed in coincidence with the low-lying transitions, from which we conclude that the bandhead is isomeric or depopulates with $\approx 25\%$ branching into one of the known isomeric states in ^{197}Pb . As mentioned in the last paragraph, the results from the DCO and gamma-ray yield ratio analysis do not seem to be consistent with an isomeric bandhead for the irregular band either.

Analysis of the DCO ratios is consistent with a stretched-dipole character for the main transitions in the two bands. In a first step a two-dimensional E_γ - E_γ matrix containing coincidences between eight detectors at angles of $37^\circ/152^\circ/154^\circ$ (x axis) and six detectors at $79^\circ/103^\circ$ (y axis) with respect to the beam axis has been sorted. This E_γ - E_γ matrix is projected on the x axis and on the y axis, respectively, while requiring the same energy gate. The intensity ratio for a particular transition observed in these two spectra, i.e., $I_\gamma(x)/I_\gamma(y)$, depends on the multipolarity of this transition and on the multipolarity of the chosen gate transition. The measured ratios of the transition intensities in the two bands together with those of the known low-lying ^{197}Pb $E2$ transitions are shown in Fig. 5. The energy gate was set on the 1006.2-keV $E2$ transition, and one sees in Fig. 5 that the DCO ratio is close to 1 for the known $E2$ transitions and close to 0.6 for the transitions in the two bands. These ratios are consistent with the expected values for $\Delta I=2$ and 1 transitions with $\delta=0$ [18] and a gate on a $\Delta I=2$ transition. The uncertainties are large because of the limited coincidence statistics in this reduced set of Ge detectors.

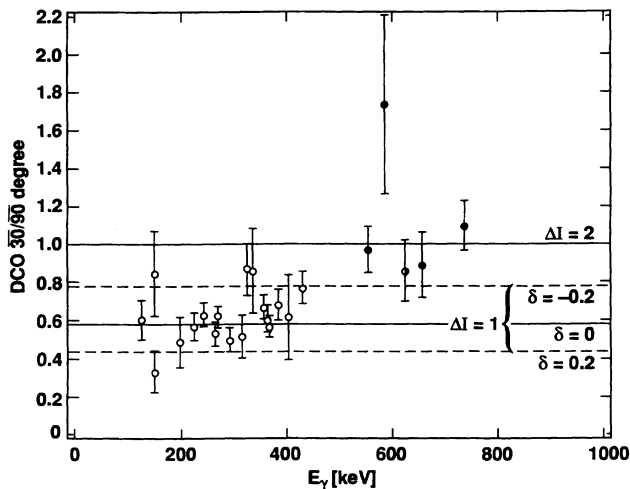


FIG. 5. DCO ratio for the transitions in the two observed bands, and for known low-lying transitions in ^{197}Pb . The energy gate is set on the 1006-keV $E2$ transition. The solid and dashed lines are the expected ratios for HERA for $\Delta I=2$ (top solid); $\Delta I=1$, $\delta=0$ (bottom solid); $\Delta I=1$, $\delta=-0.2$ (top dashed); and $\Delta I=1$, $\delta=0.2$ (bottom dashed) for a HWHM=4 for the Gaussian population of initial m states. Full circles represent $\Delta I=2$ transitions and open circles $\Delta I=1$ transitions in best agreement between the results from the DCO and Y_{\parallel}/Y_{\perp} ratios. Half-filled circles indicate an ambiguity in assignment.

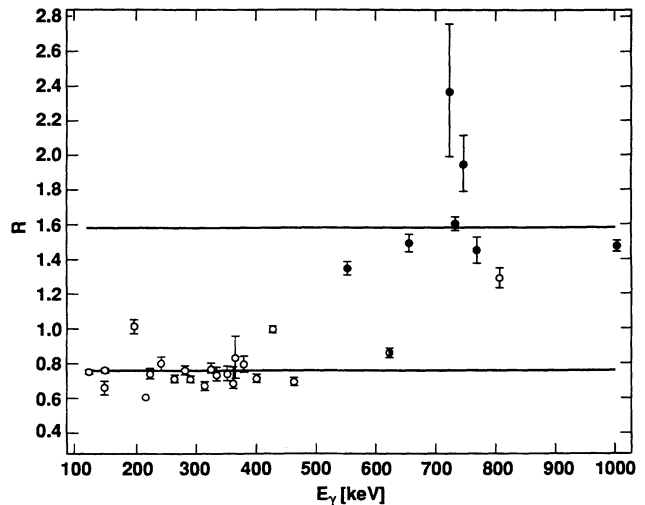


FIG. 6. The ratio Y_{\parallel}/Y_{\perp} for the low-lying transitions as well as for the members of both bands. The horizontal lines indicate the expected ratio for stretched transitions averaged over the detector angles used, and assuming full alignment. Lower line: dipoles ($I_i = \frac{3}{2} \rightarrow I_f = \frac{2}{2}$); upper line: quadrupoles ($I_i = \frac{2}{2} \rightarrow I_f = \frac{1}{2}$). Full, open, and half-filled circles same as for Fig. 5.

Therefore, we also determined R , the measured ratio Y_{\parallel}/Y_{\perp} of the γ -ray yield for a particular transition in the detectors “parallel” to the beam direction (eight detectors at angles of $\theta=37^\circ$, 152° , and 154°) to those “perpendicular” to the beam direction (six detectors at $\theta=78^\circ$ and 103°). The results of this analysis, i.e., $R = Y_{\parallel}/Y_{\perp}$, are shown in Fig. 6 together with the expected ratio for pure $\Delta I=1$ (lower line) and $\Delta I=2$ (upper line) transitions. These results are in agreement with the DCO results, and the uncertainties are much smaller. Furthermore, one has to assume $M1$ electron conversion coefficients for the strong transitions in the irregular band to obtain a reasonable intensity balance within the band and also for the low-lying transitions fed in the decay of the band (see Fig. 4). This argument does not hold for the regular band, where a reasonable intensity balance is obtained by

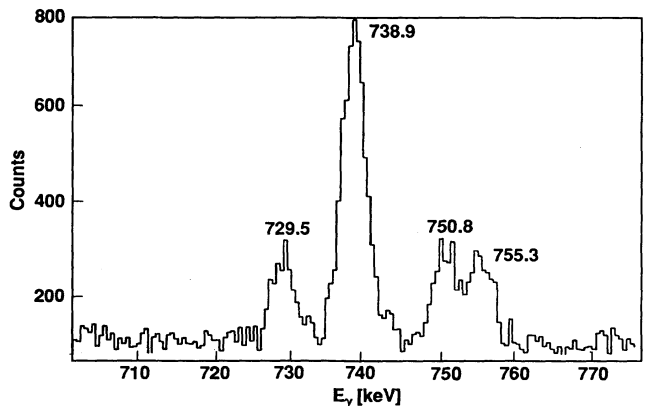


FIG. 7. Gamma-coincidence spectrum gated on the 270-keV member of the irregular band. The 729.5-, 750.8-, and 755.3-keV crossover transitions are clearly visible.

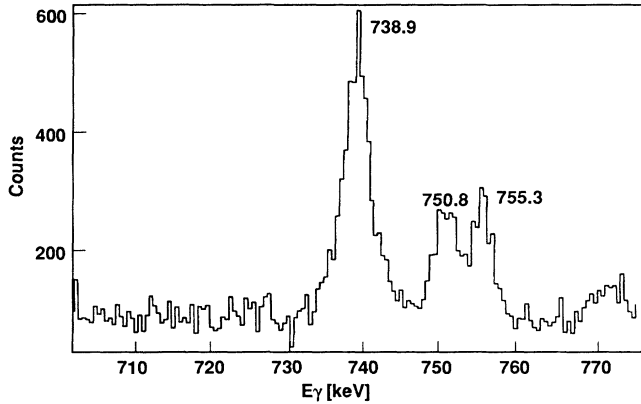


FIG. 8. Gamma-coincidence spectrum gated on the 359.2-keV member of the irregular band. The parallel 729.5-keV crossover transition is not observed.

assuming either $M1$ or $E1$ transitions. However, we have assumed $M1$ transitions in determining the indicated intensities in Fig. 2 for the regular band because the observed intensities of the low-lying members in the band and their decay into the quasiparticle states are most consistent with this assumption.

Observation of crossover transitions in both bands confirmed the relevant multipolarities deduced from the

$$B(M1)/B(E2) = 0.697 [E_\gamma(\Delta I = 2)]^5 / [E_\gamma(\Delta I = 1)]^3 \lambda (1 + \delta^2) \mu_N^2 / (e b)^2$$

with $\lambda =$ branching ratio $I_\gamma(\Delta I = 2)/I_\gamma(\Delta I = 1)$. The mixing ratio δ could not be determined accurately from the DCO ratio results (Fig. 5) because of the poor statistics, but appears to be small. We have assumed $\delta^2 \ll 1$, because the measured mixing ratios are also small in the $A = 130$ region [17] and for $^{199,200}\text{Pb}$ [16] (see text below). Therefore, the calculated values of $B(M1)/B(E2)$ represent an upper limit, and they range from 11 $\mu_N^2/(e b)^2$ to 30 $\mu_N^2/(e b)^2$ (Fig. 9).

IV. DISCUSSION

The regular structure found in ^{197}Pb is very similar to regular $\Delta I = 1$ bands observed around $A = 130$ in the odd- Z isotopes Cs, Pr, Pm, and Eu [17], in the even-even isotopes $^{126,132}\text{Ba}$ [17] as well as in $^{132,135,136}\text{Ce}$ [17] and in $^{128,130,131}\text{La}$ [17]. Recently, regular $\Delta I = 1$ bands have also been found in the neutron-deficient lead isotopes ^{198}Pb [14,15] and $^{199,200}\text{Pb}$ [16]. There are also examples for irregular bands besides the present one in ^{197}Pb : one in ^{194}Pb [10,19],² and in the neighboring nuclei $^{195,197}\text{Tl}$ [20]. Common features for a majority of these $\Delta I = 1$ bands are the following: (i) very strong $\Delta I = 1$ transitions leading to $B(M1)/B(E2)$ ratios of about 20 $\mu_N^2/e^2 b^2$ (illustrated for ^{197}Pb in Fig. 9); (ii) no signature splitting in the regular bands; (iii) low values for $\mathcal{J}^{(2)} = dI/d\omega$, the

²In the case of ^{194}Pb , the recent observation of all the $\Delta I = 2$ crossover transitions [19] led to a different order of the $\Delta I = 1$ transitions than given in [10].

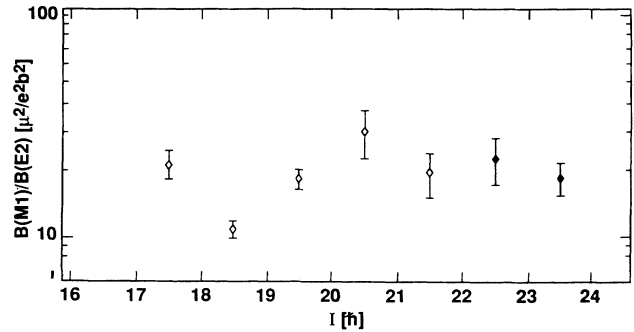


FIG. 9. $B(M1)/B(E2)$ ratios for the observed crossover transitions in the irregular (\diamond) and in the regular (\blacklozenge) band.

DCO and Y_{\parallel}/Y_{\perp} results. Spectral examples of the crossover transitions in the irregular band are shown in Figs. 7 and 8. The spectrum shown in Fig. 7 is gated on the 270-keV transition near the bottom of the irregular band and shows three crossover $E2$ transitions. In Fig. 8 the 729-keV crossover transition is not present, since the gate is on the parallel 359-keV transition. Some of the high-energy $E2$ crossover transitions for each band have been found in the data, competing with the $M1$ transitions. The crossover transitions are shown in Figs. 2 and 4. The ratio $B(M1)/B(E2)$ was calculated using

dynamic moment of inertia, except at a band crossing (illustrated for ^{197}Pb in Fig. 10); and (iv) negative $E2/M1$ mixing ratios δ for the $\Delta I = 1$ transitions in the $A = 130$ region [17] and in $^{199,200}\text{Pb}$ [16].

In the $A = 130$ region the regular $\Delta I = 1$ bands are explained as oblate, collective bands [17]. The occupation of the $h_{11/2}$ neutron orbital is considered to be the main oblate driving force for the γ -soft cores. Furthermore,

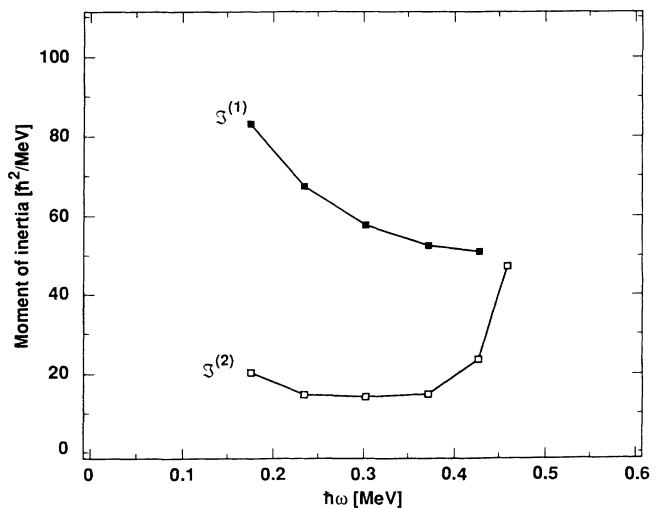


FIG. 10. Dynamic (\square) and kinematic (\blacksquare) moment of inertia for the regular band.

the occupation of the $\pi h_{11/2}(\frac{1}{2}^- [505])$ proton orbital, which is close to the Fermi surface for an oblate deformation, is considered to be responsible for the large $M1$ transition probability and for the lack of signature splitting. It has both a large K value, which accounts for a regular $\Delta I = 1$ band without signature splitting, and a large g factor ($+1.2$) [17], resulting in a large magnetic moment perpendicular to the rotation axis of the nucleus and consequently in strong magnetic-dipole transitions. The same is true for oblate, collective bands built on the known 8^+ and 11^- 2p-2h proton states in ^{196}Pb with the $\pi(\frac{1}{2}^+ [400]^{-2}, \frac{9}{2}^- [505]^2)_{8^+}$ and $\pi(\frac{1}{2}^+ [400]^{-2}, \frac{9}{2}^- [505]; \frac{13}{2}^+ [606])_{11^-}$ configurations and a measured g factor of $+0.96(8)$ for the 11^- state [9]. For $Z = 82$ these orbitals are close to the Fermi surface for an oblate deformation with $\gamma \approx -60^\circ$ and $\beta_2 \approx 0.15$ (Fig. 11).

The calculations of the neutron single-particle levels, using a deformed Woods-Saxon potential [21], show that the $\frac{3}{2}^- [512]$ and $\frac{5}{2}^- [503]$ Nilsson orbitals ($p_{3/2}$ and $f_{5/2}$ subshells, respectively) as well as the low- Ω $i_{13/2}$ orbitals approach the Fermi surface for an oblate deformation with $\beta_2 \leq -0.08$ (Fig. 11). Therefore, at proton-induced deformations near $\gamma = -60^\circ$ and $\beta_2 \approx 0.15$, the energeti-

cally favored neutron configurations in ^{197}Pb are $\nu(fp)^{1+x}(i_{13/2})^{-x}$, (Fig. 11). High-spin states related to the deformed 8^+ and 11^- states in ^{196}Pb would be formed in ^{197}Pb by coupling these neutron configurations to the oblate proton states $\pi((s_{1/2})^{-2}, (h_{9/2})^2, \text{ or } (h_{9/2}i_{13/2}))_{8^+, 11^-}$ in ^{196}Pb .

Lower limits for the bandhead excitation energies and angular momenta of the regular and irregular bands can be deduced from the available experimental data and compared with plausible estimates for the excitation energies and spins based on the simplest proton-neutron configuration for the bandheads. The experimental lower limit for the excitation energy for the bands, based on states fed by their decay, is $E_x > 3.8$ MeV for the regular band (Fig. 2) and $E_x > 3.3$ MeV for the irregular band (Fig. 4). A reasonable experimental estimate for the spin of the lowest states in the ^{197}Pb bands is $I \approx (\frac{33}{2} \pm 2)\hbar$ (regular, Fig. 2), and $I \approx (\frac{31}{2} \pm 2)\hbar$ (irregular, Fig. 4). With these experimental spin estimates, an I versus $\hbar\omega$ plot was constructed for both bands as shown in Figs. 12 and 13. In Fig. 12 the I versus $\hbar\omega$ behavior is plotted for the irregular bands in ^{197}Pb and, for comparison, in ^{194}Pb [10], and in $^{195,197}\text{Tl}$ [20]. The plots are similar for both

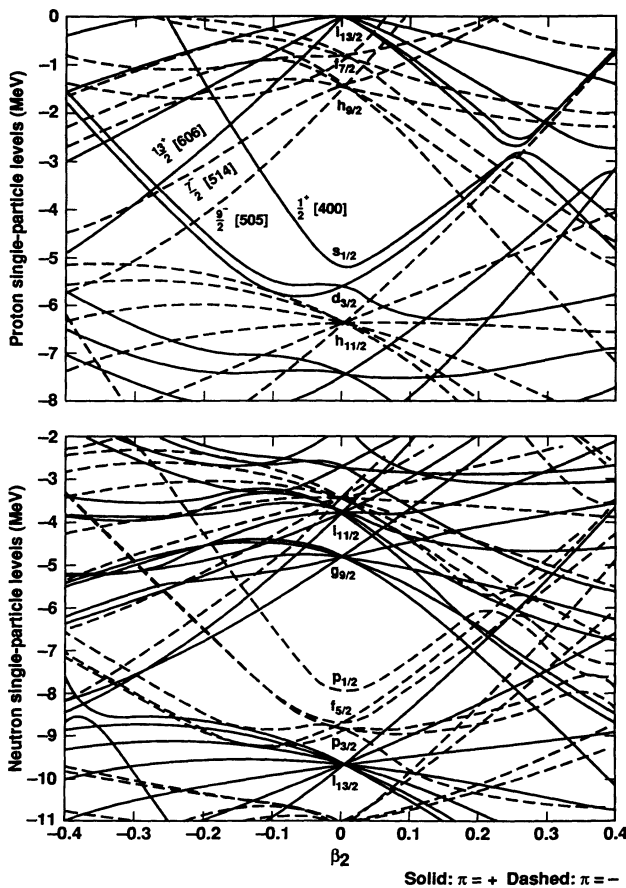


FIG. 11. Proton and neutron single-particle levels for $Z = 82$ and $N = 115$ as a function of the quadrupole deformation β_2 . Calculations were done with a deformed Woods-Saxon potential [21].

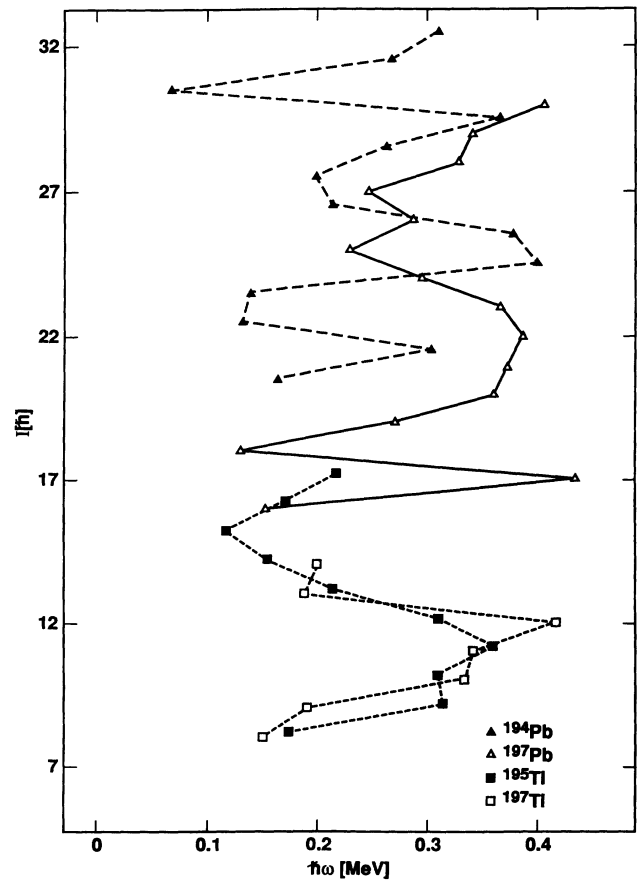


FIG. 12. Spin versus rotational frequency for the irregular band in ^{197}Pb (Δ), for the irregular band in ^{194}Pb (\blacktriangle), and for the irregular bands in ^{195}Tl (\blacksquare), ^{197}Tl (\square) [20]. The assumed spins for the levels in these bands have an uncertainty of at least $\pm 2\hbar$.

these bands. In Fig. 13 we compare the spin versus frequency behavior of the regular band in ^{197}Pb with the regular bands in ^{198}Pb [14,15] and $^{199,200}\text{Pb}$ [16]. The slope of these plots is almost the same for all of the observed regular lead bands. It is worth mentioning that the band in ^{199}Pb and band 1 in ^{200}Pb do show nearly "identical" transition energies over a large spin range [16], i.e., $E_\gamma(^{200}\text{Pb}, \text{band 1}) - E_\gamma(^{199}\text{Pb})$ is around ± 5 keV for the lowest ten transitions. It is of interest whether this similarity in transition energies is accidental or related to the systematics of the identical superdeformed bands found in the $A=150$ and 192 regions [22]. The linearly extrapolated intercept of I at $\hbar\omega=0$ is at $(15\pm 2)\hbar$ for ^{197}Pb and between $(15\pm 2)\hbar$ and $(18\pm 2)\hbar$ for the bands observed in the other lead isotopes. The intercept value is an indication of a rapid rotational alignment, considering that these bands are known down to fairly low frequency, and is indicative of low- Ω , high- j orbitals (probably $i_{13/2}$ orbitals).

A plausible excitation energy for the bandheads of the two bands in ^{197}Pb , based on the simplest neutron configuration coupled to the oblate 8^+ and 11^- states seen in ^{196}Pb , i.e., $\pi(2p-2h)\otimes\nu(fp)^2(i_{13/2})^{-1}$, should be similar to the excitation energy for the $\frac{33}{2}^+$ state at

$E_x \approx 3.1$ MeV in ^{197}Pb . The $\frac{33}{2}^+$ state has been explained to have a $\nu(fp)^4(i_{13/2})^{-3}$ configuration [6], i.e., $\nu(fp)^2(i_{13/2})^{-1}$ coupled to the $\nu(fp)^2(i_{13/2})^{-2}$ 12^+ states in ^{196}Pb [8], which is found close to the $\pi(2p-2h) 8^+$, and $\pi(2p-2h) 11^-$ states, respectively, in ^{196}Pb . Therefore, we expect an oblate state in ^{197}Pb , with the above-mentioned configuration, close to an excitation energy of $E_x = 3.1$ MeV. However, coupling only one low- Ω $i_{13/2}$ neutron hole to the high- Ω proton orbitals, i.e., oblate 8^+ and 11^- states, results in a total spin $I \approx \frac{21}{2}$ and $\frac{25}{2}$, respectively, for the resulting states, because the proton and neutron spins are roughly perpendicular to each other. The experimentally observed spins can be obtained only if the bands are built on states for which at least two $\nu i_{13/2}$ quasiparticles couple to the proton 11^- state, i.e., $I[\pi(11^-)\otimes\nu(fp)^3(i_{13/2})^{-2}] \approx \frac{31}{2}$. According to the calculations of the neutron single-particle energies at a deformation of $\gamma = -60^\circ$ and $\beta_2 \approx 0.15$ (Fig. 11, $\beta_2 \approx -0.15$) the energy necessary to produce more than one $i_{13/2}$ neutron hole is relatively small, i.e., it is still reasonable to expect states with more than one $i_{13/2}$ quasiparticle involved near 3.1-MeV excitation energy. In fact, the rapid alignment of $i \approx (15\pm 2)\hbar$ determined for the regular band from the plot in Fig. 14 may suggest that at least three $\nu i_{13/2}$ quasiparticles are involved in the bandhead configuration for the regular band. In Fig. 14 we show the neutron single-particle Routhians as a function of $\hbar\omega$ for the Nilsson-orbitals involved. According to these calculations the energetically favored state at $\hbar\omega \approx 0.45$, and neutron numbers $112 \leq N \leq 118$, involves two, three, or four holes in the $\nu i_{13/2}$ subshell. The alignment $i = -de/d\omega$ for these $i_{13/2}$ Nilsson orbitals, determined from Fig. 14, is $i = 6, 5, 3$, and 2.7 for holes in the $i_{13/2}$ ($\Omega = \frac{1}{2}$ and $\frac{3}{2}$) orbitals. This can generate the experimentally found values of $i \approx (15\pm 2)\hbar$ for the rapid initial alignment in the ^{197}Pb regular band.

Thus, one possible configuration for the regular band is $\pi(11^-)\otimes\nu(fp)^4(i_{13/2})^{-3}$. From the single-particle

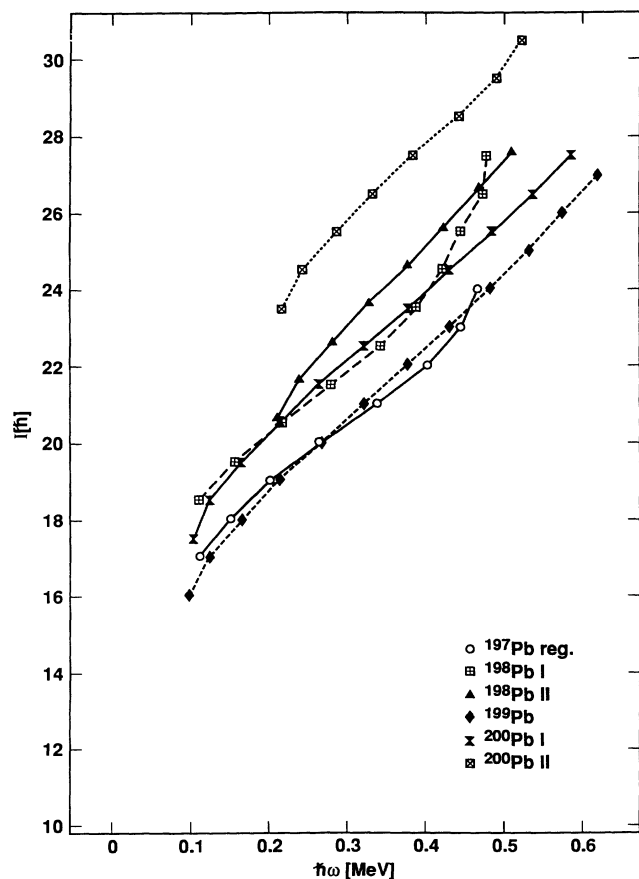


FIG. 13. Spin versus rotational frequency for the regular band in ^{197}Pb (\circ), bands I (\square) and II (\triangle) in ^{198}Pb [14,15], the band in ^{199}Pb (\diamond) [16], and bands I (\times) and II (\boxtimes) in ^{200}Pb [16]. The assumed absolute spins for these bands have an uncertainty of at least $\pm 2\hbar$.

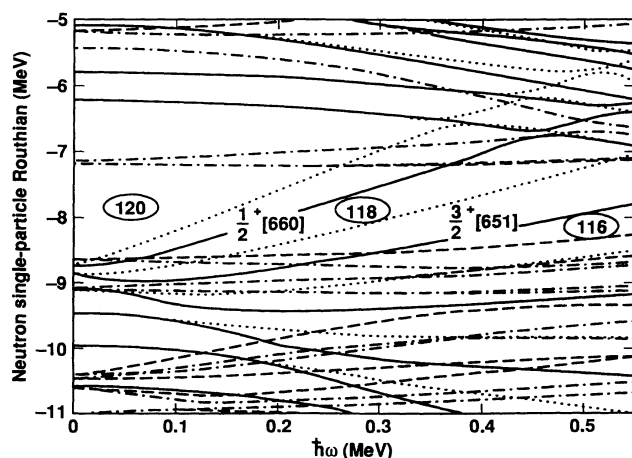


FIG. 14. Neutron single-particle Routhians as a function of rotational frequency $\hbar\omega$ for $N=115$, $\beta_2=0.15$, $\beta_4=0$, and $\gamma=-60^\circ$.

Routhians (Fig. 14) we obtain an alignment of $14\hbar$ $[(6+5+3)\hbar]$ for this configuration. The similar I versus ω behavior of the regular bands in the even- N $^{198,200}\text{Pb}$ and odd- N $^{197,199}\text{Pb}$ nuclei (Fig. 13) suggests the same configuration for all of these regular bands. This is in contradiction to the interpretation of these bands as having a $\pi(11^-) \otimes \nu(fp)^x(i_{13/2})^{-2}$ bandhead configuration for the even- N $^{198,200}\text{Pb}$ isotopes [14,16], and more work is necessary to resolve the configuration.

The irregular band, which is found at a lower excitation energy, shows the following characteristics of a collective band: (1) the spins are in sequence ($\Delta I=1$) and (2) the observed $B(M1)/B(E2)$ ratios are large in the whole γ -ray sequence. However, it seems not to be a typical collective band because of the strong irregularities seen in the I versus $\hbar\omega$ plot (Fig. 12), but it does not look completely noncollective either. There is a strong resemblance between the two irregular structures found so far in ^{194}Pb and ^{197}Pb . There are somewhat similar bands observed in $^{195,197}\text{Tl}$ [20]. We cannot give a detailed explanation for the mechanism leading to this irregular band, but we suggest that one possibility is a triaxial rotational band built on the same general configuration as suggested for the regular bands, or that the irregular band has a smaller β deformation because of a somewhat different configuration. Clearly more data and calcula-

tions are needed to solve this problem.

A better understanding of the quasiparticle configurations involved can be obtained from a study of the total Routhians surface (TRS) for the above-mentioned proton configuration and for the possible neutron configurations. The unambiguously established spin and parity $I^\pi=11^-$ for the proton 2p-2h state in the $^{194,196}\text{Pb}$ isotopes [9,10] confirms the occupation of the $\frac{9}{2}^- [505]_{1/2}^+ + [606]$ Nilsson orbitals even though the $\frac{7}{2}^- [514]$ orbital is lower in energy than the $\frac{13}{2}^+ [606]$ orbital (see Fig. 11). The TRS calculation [23] (Fig. 15) shows at low ω a minimum at $\gamma = -72^\circ$ and $\beta_2 \approx 0.1$. For low rotational frequency the deformation is γ soft, but it stabilizes at $\gamma \approx -65^\circ$ for $0.28 \text{ MeV} \leq \hbar\omega \leq 0.45 \text{ MeV}$.

For the neutrons, the TRS has been extracted from the available mesh [23] for the one-quasiparticle configuration, i.e., $\nu i_{13/2}(\frac{1}{2}^+ [600]^{-1})$ and, for the three-quasiparticle configuration, i.e., $\nu i_{13/2}(\frac{1}{2}^+ [600]^{-2}; \frac{3}{2}^+ [651]^{-1})$. The results of these calculations are almost the same for both configurations, and we show them for the three-neutron quasiparticle configuration in Fig. 16. Both configurations have an energy minimum at low frequencies at a very small deformation of $\beta_2 \approx 0.06$ and $\gamma \approx -60^\circ$, therefore providing a stabilizing effect for the proton-induced deformation. This is seen by comparing Figs. 15 and 16 with Fig. 17, which shows the TRS calculation [23] for the neutron-proton configuration pro-

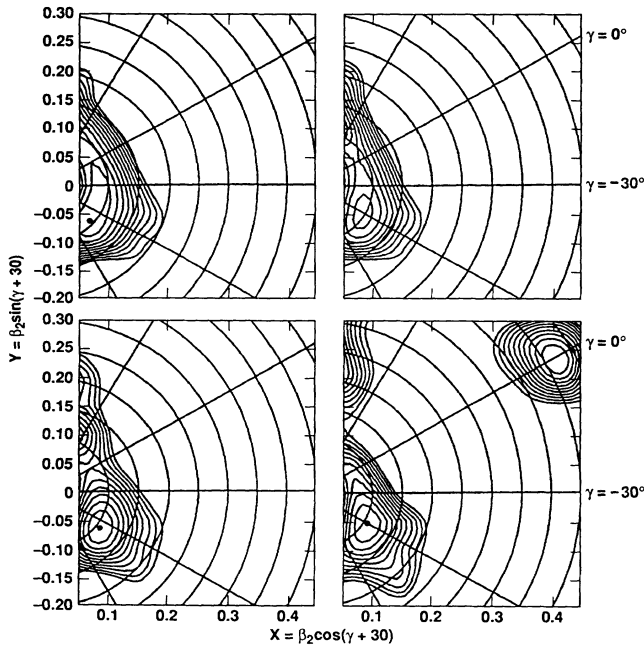


FIG. 15. TRS maps [23] for the $\pi(\frac{1}{2}^+[400]^{-2}; \frac{9}{2}^- [505]; \frac{13}{2}^+[606])_{11^-}$ configuration. The energy E , quadrupole deformation parameter β_2 , triaxiality parameter γ , and rotational frequency ω are given for the minimum. For certain values of ω it moves to $\gamma > 0$, but we focus on what happens around $\gamma = -60^\circ$. Top left: $E = -1.44 \text{ MeV}$, $\gamma = -72.2^\circ$, $\beta_2 = 0.093$, $\omega = 0.05$. Top right: $E = -2.95 \text{ MeV}$, $\gamma = +37.2^\circ$, $\beta_2 = 0.114$, $\omega = 0.17$. Bottom left: $E = -5.04 \text{ MeV}$, $\gamma = -66.8^\circ$, $\beta_2 = 0.107$, $\omega = 0.28$. Bottom right: $E = -9.98 \text{ MeV}$, $\gamma = -60.0^\circ$, $\beta_2 = 0.106$, $\omega = 0.44$.

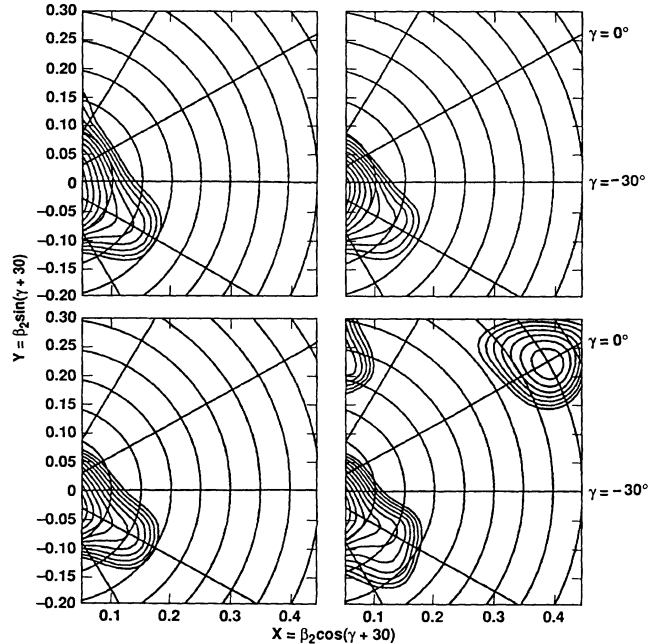


FIG. 16. TRS maps [23] for the $\nu(\frac{1}{2}^+[660]^{-2}; \frac{3}{2}^+[651]^{-1})$ configuration. The energy E , quadrupole deformation parameter β_2 , triaxiality parameter γ , and rotational frequency ω are given for the minimum. Top left: $E = -5.36 \text{ MeV}$, $\gamma = -66.8^\circ$, $\beta_2 = 0.06$, $\omega = 0.05$. Top right: $E = -7.14 \text{ MeV}$, $\gamma = -49.2^\circ$, $\beta_2 = 0.05$, $\omega = 0.17$. Bottom left: $E = -13.32 \text{ MeV}$, $\gamma = -67.5^\circ$, $\beta_2 = 0.06$, $\omega = 0.32$. Bottom right: $E = -11.61 \text{ MeV}$, $\gamma = -70.0^\circ$, $\beta_2 = 0.06$, $\omega = 0.44$.

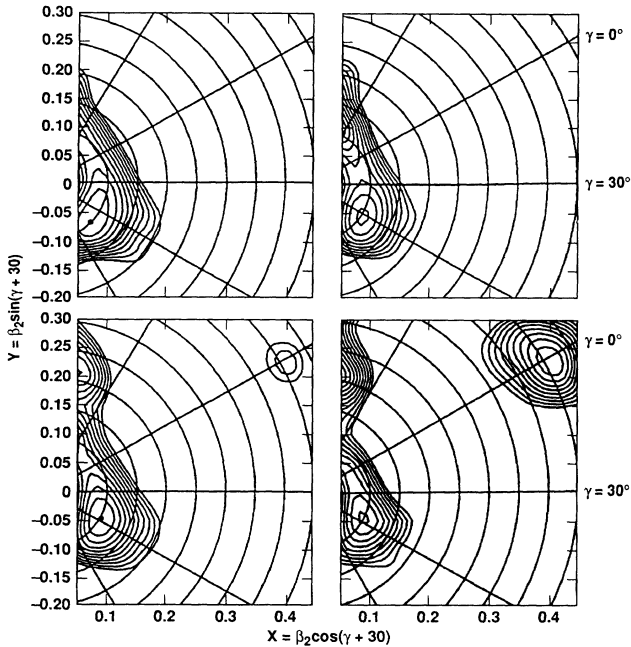


FIG. 17. TRS maps [23] for the proposed proton-neutron configuration. The energy E , quadrupole deformation parameter β_2 , triaxiality parameter γ , and rotational frequency ω are given for the minimum. For certain values of ω it moves to $\gamma > 0$, but we focus on what happens around $\gamma = -60^\circ$. Top left: $E = -0.16$ MeV, $\gamma = -73.7^\circ$, $\beta_2 = 0.10$, $\omega = 0.05$. Top right: $E = -3.74$ MeV, $\gamma = +37.1^\circ$, $\beta_2 = 0.11$, $\omega = 0.24$. Bottom left: $E = -6.33$ MeV, $\gamma = -67.5^\circ$, $\beta_2 = 0.10$, $\omega = 0.36$. Bottom right: $E = -9.41$ MeV, $\gamma = +48.0^\circ$, $\beta_2 = 0.21$, $\omega = 0.44$.

posed for the regular band, i.e.,

$$\pi\left(\frac{1}{2}^+[400]^{-2}, \frac{9}{2}^-[505]; \frac{13}{2}^+[606]\right) \\ \otimes \nu i_{13/2}\left(\frac{1}{2}^+[660]^{-2}, \frac{3}{2}^+[651]^{-1}\right).$$

The oblate minimum is less γ soft already at low rotational frequencies for the suggested proton-neutron configuration.

At higher frequencies of $\hbar\omega > 0.45$ MeV the minimum for the low- Ω $i_{13/2}$ orbitals becomes more γ soft towards $\gamma \approx -90^\circ$. This is eventually seen in the experimental data for the regular bands in ^{197}Pb , ^{198}Pb , band 1 [15], and ^{200}Pb , band 2 [16]. For these bands one observes a sharp decrease in ΔE_γ (upbend in Fig. 13) for transition energies above 400 keV.

Additionally, the total Routhians surfaces for the $p_{3/2}$ and $f_{5/2}$ orbitals have been extracted. According to these TRS calculations [23] an increased γ softness occurs for the $p_{3/2}$ and $f_{5/2}$ Nilsson orbitals for $\hbar\omega \geq 0.2$ MeV. This result supports the single-particle and quasi-particle calculations showing that these orbitals could drive the ^{197}Pb nucleus towards a triaxial shape, i.e., $-120^\circ < \gamma < -60^\circ$. However, it is not yet clear whether the occupation of these orbitals is responsible for the appearance of irregular bands in the $N \leq 115$ lead nuclei. Thus, a more specific configuration, based on these calcu-

lations, cannot be assigned for their bandheads.

The proposed configurations for the bandheads are based on the data available. However, more experimental data are needed, particularly on linking transitions to the low-lying states, in order to establish the spin and excitation energy of the bandheads. The overall trend of these $\Delta I = 1$ bands in the neutron-deficient lead isotopes shows a transition from irregular to more regular structures with increasing neutron number from $N = 112$ to 118. Thus far the nucleus ^{197}Pb is the only one where both a regular and an irregular collective band are known, as discussed here. The calculations for the quasineutron Routhians as a functions of γ have also been done for neutron numbers $112 \leq N \leq 118$ at $\beta_2 = 0.15$ and $\hbar\omega = 0.2$ MeV in order to understand this transition from irregularity to regularity for $N = 115$. These calculations indicate shallower energy minima around $\gamma = -60^\circ$ for the involved $\nu i_{13/2}$ orbitals with decreasing neutron number from $N = 118$ to 112. The involved $\nu p_{3/2}$ and $\nu f_{5/2}$ orbitals, which are almost flat as a function of γ for $N = 118$, start to develop minima at $-120^\circ \leq \gamma \leq -100^\circ$ for $N \leq 116$. However, for $N = 116$ the $\nu i_{13/2}$ orbitals still have a dominant minimum around $\gamma = -60^\circ$. This situation changes for $N \leq 115$. For these neutron numbers the $\nu i_{13/2}$ orbitals become more flat for γ between -60° and -100° , and the prolate noncollective (towards $\gamma = -120^\circ$) driving $p_{3/2}$ and $f_{5/2}$ orbitals become dominant.

V. SUMMARY

The partial level scheme of ^{197}Pb has been extended up to a spin of approximately $\frac{62}{2}\hbar$ and an excitation energy of at least 8 MeV. The new data for ^{197}Pb are dominated by two collective bands with fast dipole transitions. Similar bands have also been observed in other lead isotopes ^{194}Pb [10], ^{196}Pb [9], ^{198}Pb [14,15], and $^{199,200}\text{Pb}$ [16]. These bands are interpreted as evidence of a collective rotation of an oblate-deformed ^{197}Pb nucleus. A possible explanation of the bandhead configuration, based on experimentally observed properties, has been advanced. Further detailed experimental studies are necessary to establish the linking transitions between the bands and the low-lying states providing bandhead spins and energies. These data would, together with further theoretical studies, permit a confirmation of the proposed bandhead configurations.

ACKNOWLEDGMENTS

We wish to thank Prof. Dr. H. Hübel for discussing and releasing his results on similar $\Delta I = 1$ bands in ^{199}Pb and ^{200}Pb prior to publication. This work was supported in part by the U.S. Department of Energy under Contract No. W-7405-ENG-48 (LLNL), in part by the Office of Energy Research, Division of Nuclear Physics of the Office of High Energy and Nuclear Physics of the U.S. Department of Energy under Contract No. DE-AC03-76SF00098 (LBL), and in part by the National Science Foundation (Rutgers).

- [1] E. F. Moore *et al.*, Phys. Rev. Lett. **63**, 360 (1989).
- [2] J. A. Becker, N. Roy, E. A. Henry, M. A. Deleplanque, C. W. Beausang, R. M. Diamond, J. E. Draper, F. S. Stephens, J. A. Cizewski, and M. J. Brinkman, Phys. Rev. C **41**, R9 (1990), and D. Ye *et al.*, Phys. Rev. C **41**, R13 (1990).
- [3] A list of references is given in J. A. Becker *et al.*, submitted to Phys. Rev. C.
- [4] R. V. F. Janssens and T. L. Khoo, Annu. Rev. Part. Nucl. Sci. **41**, 321 (1991).
- [5] Preliminary results presented at the APS spring meeting in Washington, D.C., 1991.
- [6] M. Pautrat, J. M. Lagrange, J. S. Dionisio, Ch. Vieu, and J. Vanhorenbeck, Nucl. Phys. **A443**, 172 (1985).
- [7] P. Van Duppen, E. Coenen, K. Deneffe, M. Huyse, K. Heyde, and P. Van Isacker, Phys. Rev. Lett. **52**, 1974 (1984).
- [8] J. J. Van Ruyven, J. Penninga, W. H. A. Hesselink, P. Van Ness, K. Allaart, E. J. Hengeveld, H. Verheul, M. J. A. De Voigt, Z. Sujkowski, and J. Blomqvist, Nucl. Phys. **A449**, 579 (1986).
- [9] J. Penninga, W. A. H. Hesselink, A. Balanda, A. Stolk, and H. Verheul, Nucl. Phys. **A471**, 535 (1987).
- [10] B. Fant *et al.*, J. Phys. G. **17**, 319 (1991).
- [11] K. Heyde *et al.*, Phys. Rep. **102**, 291 (1983).
- [12] S. Frauendorf *et al.*, *Future Directions in Studies of Nuclei far from Stability*, edited by J. H. Hamilton (North-Holland, Amsterdam, 1983), p. 133.
- [13] B. Bengtsson and W. Z. Nazarewicz, Z. Phys. **334**, 269 (1989).
- [14] R. M. Clark *et al.*, Phys. Lett. B **275**, 247 (1992).
- [15] T. F. Wang *et al.*, submitted to Phys. Rev. Lett.
- [16] H. Hübel, Wetherill Symposium, Philadelphia, 1991 (unpublished); G. Baldsiefen *et al.*, Phys. Lett. B **275**, 252 (1992).
- [17] D. B. Fossan, J. R. Hughes, Y. Liang, R. Ma, E. S. Paul, and N. Xu, Nucl. Phys. **A520**, 241c (1990), and references therein.
- [18] J. E. Draper, Nucl. Instrum. Methods A **247**, 481 (1986).
- [19] M. J. Brinkman, Ph.D. dissertation, Rutgers University, 1991; and M. J. Brinkman *et al.* (unpublished).
- [20] R. M. Kieder, A. Neskakis, M. Müller-Veggian, Y. Gono, C. Meyer-Böricke, S. Beshai, K. Fransson, C. G. Linden, and Th. Lindblad, Nucl. Phys. **A299**, 255 (1978).
- [21] S. Cwiok, J. Dudek, W. Nazarewicz, J. Skalski, and T. Werner, Comput. Phys. Commun. **46**, 379 (1987).
- [22] F. S. Stephens *et al.*, Phys. Rev. Lett. **64**, 2623 (1990), and references therein.
- [23] R. Wyss, W. Satula, W. Nazarewicz, and A. Johnson, Nucl. Phys. **A511**, 324 (1990).